ANL/ET/CP--86419

CONF-950961--9

Effect of Oxygen and Oxidation on Tensile Properties of V-5Cr-5Ti Alloy*

K. Natesan and W. K. Soppet
Energy Technology Division
Argonne National Laboratory
Argonne, IL 60439, U.S.A.
Tel: (708) 252-5103
Fax: (708) 252-3604

RECEIVED

FEB 08 1996

OSTI

September 1995

MASTER

DISTRIBUTION OF THIS DOCUMENT IS UNLIMITED

Effect of Oxygen and Oxidation on Tensile Properties of V-5Cr-5Ti Alloy[*]

K. Natesan and W. K. Soppet
Energy Technology Division
Argonne National Laboratory
Argonne, IL 60439, U.S.A.

Oxidation studies were conducted on V-5Cr-5Ti alloy specimens in an air environment to evaluate the oxygen uptake behavior of the alloy as a function of temperature and exposure time. The oxidation rates calculated from parabolic kinetic measurements of thermogravimetric testing and confirmed by microscopic analyses of cross sections of exposed specimens were 5, 17, and 27 µm per year after exposure at 300, 400, and 500°C, respectively. Uniaxial tensile tests were conducted at room temperature and at 500°C on preoxidized specimens of the alloy to examine the effects of oxidation and oxygen migration on tensile strength and ductility. Microstructural characteristics of several of the tested specimens were determined by electron optics techniques. Correlations were developed between tensile strength and ductility of the oxidized alloy and microstructural characteristics such as oxide thickness, depth of hardened layer, depth of intergranular fracture zone, and transverse crack length.

Introduction

Refractory alloys in general and vanadium alloys in particular are susceptible to pickup of interstitials such as oxygen, carbon, and nitrogen, which can affect the short- and long-term mechanical properties of the materials. The vanadium alloy with a composition of V-5Cr-5Ti contains 5 wt.% titanium (a much more stable oxide-former than vanadium and chromium), which can have an even stronger effect on mechanical properties, especially on tensile and creep ductility. The degree of influence of interstitials such as oxygen on the alloy's properties will be dictated by alloy grain size (the amount of grain-boundary areas), amount and distribution of oxygen in the alloy, amount and size of second-phase oxide precipitates (such as titanium oxide), service temperature and time of exposure. The purpose of this study is to examine the role of oxygen and oxidation rate on tensile properties of the alloy.

Experimental Procedure

The heat of vanadium alloy selected for the study (designated as BL-63) had a nominal composition of V-5 wt.%Cr -5 wt.%Ti; actual composition is given in Table 1. A sheet material of the alloy was annealed for 1 h at 1050°C prior to its use in oxidation and tensile testing. Coupon specimens measuring ≈15 x 7.5 x 1 mm were used for the oxidation studies. Oxidation experiments were conducted in air in a thermogravimetric test apparatus at temperatures between 300 and

650°C. The temperatures were maintained within ±2°C of the desired value.

Tensile specimens were fabricated according to ASTM specifications and had a gauge length of ≈19 mm and a gauge width of ≈4.5 mm. The grain size of the specimens was ≈32 μm. The specimens were preoxidized in air at 500°C for 24, 250, 600, 1000, and 2060 h prior to tensile testing in air at 500°C. Similar specimens preoxidized up to 1000 h at 500°C in air were also tensile tested at room temperature. As-annealed (control) specimens were tensile tested on an Instron machine at constant crosshead speeds between 0.0005 and 0.2 cm/min. These speeds correspond to initial strain rates in the range of 4.4×10^{-6} to 1.8×10^{-3} s^{-1}. The preoxidized specimens were tested at a strain rate of 1.8×10^{-4} s^{-1}. The test temperature was maintained within 2°C in all tests performed in air at 500°C. The specimens were loaded by means of pins that pass through holes in the grips and enlarged end sections of the specimen, thus minimizing misalignment. Total elongation was measured with a vernier caliper and by using load/elongation chart records. The fracture surfaces, longitudinal and axial cross sections of tested specimens were examined by scanning electron microscopy (SEM). In addition, Vickers hardness was measured on several of the tested specimens. Coupon specimens of the alloy that were oxidized with the tensile specimens were analyzed for bulk oxygen content by a vacuum-fusion technique.

Results and Discussion

Oxidation Behavior

Figure 1 shows weight change data for the alloy oxidized in air at several temperatures. The oxidation kinetics followed a parabolic relationship with time. Detailed SEM analysis (with both energy-dispersive and wavelength-dispersive analysis) of the oxidized samples showed that the outer layer was predominantly vanadium-rich oxide and the inner layer was (V,Ti) oxide. Further, X-ray diffraction data of the oxides showed the outer oxide to be V_2O_5; and no nitrogen or nitride phases were detected. The thickness of the oxide scale of the specimens calculated from a parabolic rate equation was in good agreement with the values determined by microscopy. Secondary on mass spectrometry (SIMS) technique was used to obtain depth profile for oxygen in the tested specimens. Figure 2 shows the scale thickness (calculated on the basis of parabolic kinetics) after a 1-yr exposure in air as a function of exposure temperature in the range of 300-575°C. The results show that scale thicknesses were 5, 10, 17, and 27 μm after the 1-year exposure in air at 300, 400, 450, and 500°C, respectively. Even though the oxide thicknesses are small at these temperatures, the alloy also exhibits an oxygen-enriched region, ahead of the oxide scale, which can lead to hardening of the material and may also embrittle the alloy. Figure 3 shows the surface-to-interior Vickers hardness profile of specimens exposed to air for various times at 500°C. The oxide scale thickness is ≈10 μm but a hardness increase is noted to a depth of up to 120 μm, indicating an oxygen-enriched zone ahead of the oxide scale.

Baseline Tensile Properties

Engineering stress/engineering strain curves were developed from load-elongation data that was based on the initial cross sectional area of the specimen. Figure 4 shows the stress/strain curves for as-annealed (control) specimens tested at various strain rates. The data show negligible effect of strain rate on the yielding phenomenon and on yield stress at 500°C. The tensile ductility of the alloy was in a range of 0.21-0.24 over the strain rates used in this study. The maximum engineering stress increased with a decrease in strain rate and was $\approx$460 and 392 MPa at strain rates of 4.3 x 10^{-6} and 1.8 x 10^{-3} s^{-1}, respectively. The variation in maximum engineering stress with strain rate can be described by the relationship

$$UTS(MPa) = 319 - 24.4\log\dot\varepsilon,$$

where UTS is ultimate tensile strength in MPa and $\dot\varepsilon$ is strain rate.

Effect of Oxidation on Tensile Properties

To evaluate the effect of oxide scale formation and oxygen penetration into the substrate alloy, the tensile behavior of the alloy was examined as a function of oxygen ingress and oxide scale formation. Tensile specimens were exposed to air for 24-2060 h in air at 500°C and then tensile tested in air at either room temperature or 500°C. All oxidized specimens were tested at a strain rate of 1.8 x 10^{-4} s^{-1}.

Figure 5 shows the engineering stress/engineering strain curves at 500°C for specimens after oxidation for several exposure times in the range of 0-2060 h. The data indicate that the stress/strain behavior of the alloy is virtually unaffected by 24 h exposure in air at 500°C. As the exposure time increases to 250 h, the strength of the alloy increases with some loss in tensile ductility. In the exposure period of 250-1000 h, the alloy essentially has the same ultimate tensile strength but with reductions in tensile ductility from 0.21 at 24 h exposure to 0.14 at 1000 h exposure. Further exposure of the alloy to air at 500°C results in loss of strength and tensile ductility, as evidenced by the stress/strain curve for the specimen preoxidized for 2060 h.

Figure 6 shows the engineering stress/engineering strain curves obtained at room temperature for specimens after oxidation for several exposure times in the range of 0-1000 h. The data indicate a significant increase in tensile strength of the alloy after 24 h of oxidation. The rupture strain of the specimen decreased from $\approx$0.32 to 0.265 after 24 h of oxidation at 500°C. However, the effect of oxidation on ductility was more severe as the time of oxidation increased to 260 h and beyond. The rupture strain values were, respectively 0.07, 0.032, and 0.032 after 260, 600, and 1000 h of oxidation. Figures 7 and 8 show the variations in maximum engineering stress and rupture strain as a function of preoxidation time in air at 500°C for tests conducted at room temperature and 500°C.

Microstructural Observations

Axial cross sections of several of the tested specimens were examined by SEM. Figure 9 shows specimen sections tested in as-annealed condition and after oxidation for 24, 250, 1000, and 2060 h in air at 500°C. The photomicrographs show that as oxidation time increases, both cracks in the transverse direction and the crack spacing in the axial direction increase. Furthermore, as the oxidation time increases, the specimen undergoes little necking of the gage section during the tensile test. It is evident, especially from specimens exposed for 1000 and 2060 h, that fracture occurred by propagation of one of the axial cracks and that because the core of the alloy was somewhat ductile, the crack-propagation direction in the core region was at an angle of $\approx45°$.

Figure 10 shows photomicrographs of as-annealed and preoxidized specimens tested at room temperature. The as-annealed specimen exhibited significant necking prior to fracture. The specimen preoxidized for 24 h exhibited numerous cracks and showed reduced necking when compared with the as-annealed specimen. The specimen preoxidixed for 260 h exhibited several small cracks but showed virtually no necking prior to fracture. The specimens preoxidized for 600 and 1000 h showed no surface cracks but the specimens were fully embrittled.

Figure 11 shows SEM photomicrographs of fracture surfaces of specimens tested at 500°C in as-annealed condition and after oxidation for several time periods. The fracture mode was predominantly ductile in the as-annealed specimen. The specimen exposed for 24 h to air at 500°C showed a layer of grain-boundary or cleavage morphology for a depth of ≈25 μm, beyond which a ductile fracture mode was observed. With increases in oxidation time, the zone of intergranular fracture increased and, for the 2060-h-oxidized specimen, the depth of this zone was 165 μm.

Figure 12 shows the SEM photomicrographs of fracture surfaces of specimens tested at room temperature in as-annealed condition and after oxidation for several time periods. It is evident that the as-annealed specimen exhibited fully ductile fracture, whereas the 24-h preoxidized specimen showed partially ductile fracture. The specimens preoxidized for 260 h or longer exhibited completely intergranular fracture over the entire cross section, indicating that oxygen enrichment, even in the center of these specimens, is sufficient to fully embrittle the alloy. At present, efforts are underway to establish the threshold oxygen level for transition from ductile to brittle mode of fracture.

Table 2 lists the calculated and measured thickness of oxide layers, depths of hardened layers (from Vickers hardness measurements), thickness of intergranular fracture zones, and transverse crack lengths for specimens as-annealed and preoxidized and tensile tested at room temperature and 500°C. The data in Table 2 show that the oxide layer is fairly thin even after exposure to air at 500°C for 2060 h. However, oxygen diffusion into the substrate alloy and its enrichment in the surface regions of the specimens alter the fracture mode, changing it from ductile to cleavage. Furthermore, the thickness of the zone of intergranular fracture is in good agreement with the crack lengths measured in

the transverse direction. The difference in the intergranular fracture zone thickness and the crack length can be attributed to a subsurface oxygen-enriched layer that is not fully brittle. The results also indicate that there is a threshold oxygen concentration in the alloy for embrittlement to ensue and this aspect is presently being investigated.

Figure 13 shows variations in the hardened layer, intergranular fracture zone thickness, and transverse crack length as a function of oxidation time for specimens tested at 500°C. Tensile rupture strain values are also shown in the figure. Results to date indicate that oxygen ingress (from oxidation in air) into the material leads to catstrophic embrittlement of the alloy at room temperature but the alloy exhibits some ductility at 500°C. Additional exposures as a function of oxygen partial pressure in the exposure environment, as well as tensile tests at other temperatures on oxidized specimens, are in progress to establish alloy performance in an oxygen-containing environment.

Summary

Oxidation studies were conducted on V-5Cr-5Ti alloy specimens at several temperatures in an air environment. The oxidation process followed a parabolic rate law. The oxide scale exhibited a dual layer, with the outer layer predominantly vanadium oxide and the inner layer (V,Ti) oxide. Tensile specimens were preoxidized for times ranging from 24 to 2060 h in air at 500°C, and were subsequently tensile tested at either room temperature or 500°C. The effect of oxidation on the stress/strain behavior of the alloy was evaluated. The propensity of the alloy to fracture and cracking upon oxidation was analyzed and correlated with hardness, fracture morphology, and rupture strain.
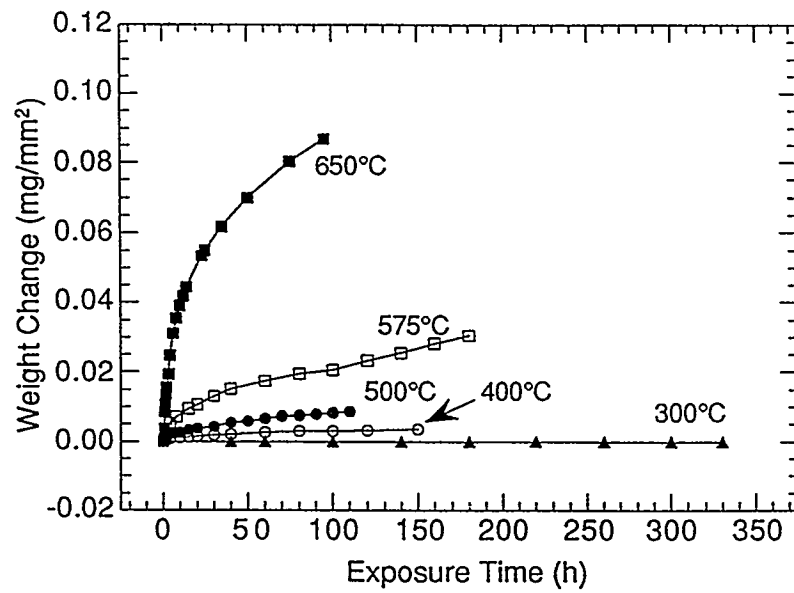
Acknowledgments

Figure 1. Weight change data for oxidation of V-5Cr-5Ti
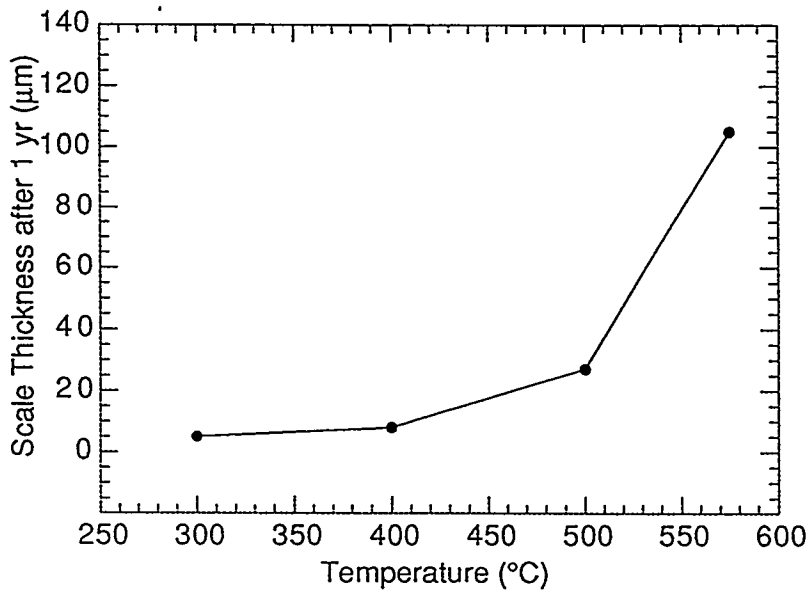alloy in air at several test temperatures.

Figure 2. Oxide scale thickness for V-5Cr-5Ti alloy in air
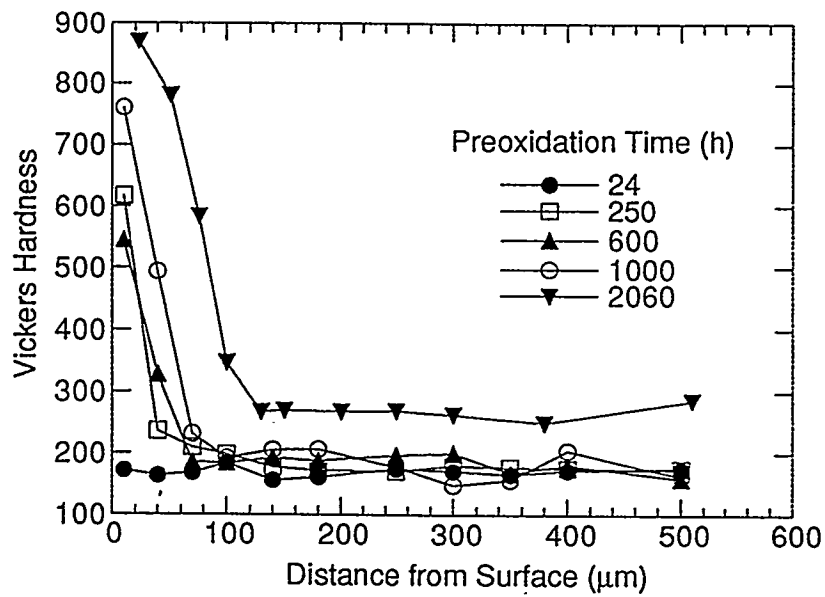as a function of exposure temperature.

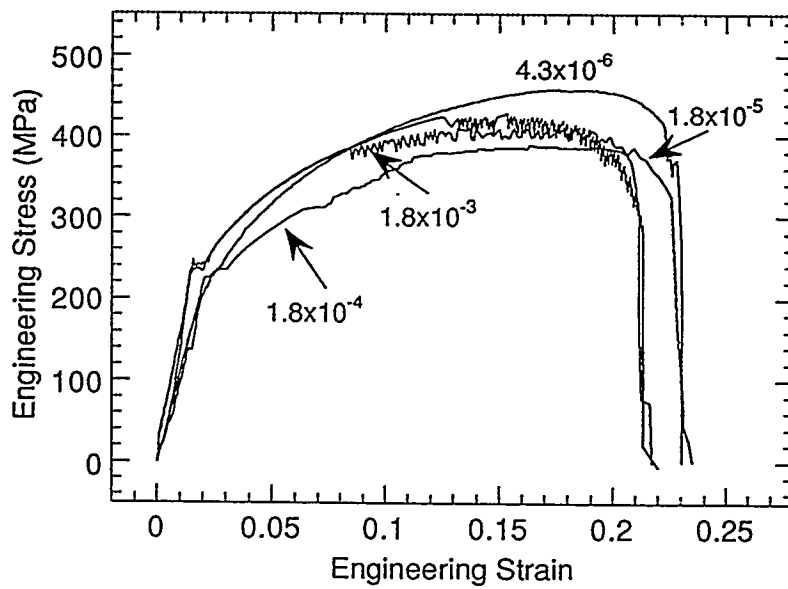Figure 3. Vickers hardness data for specimens of V-5Cr-5Ti alloy oxidized at 500°C in air for various times.

Figure 4. Stress-strain behavior of V-5Cr-5Ti alloy tested at 500°C in air at several strain rates
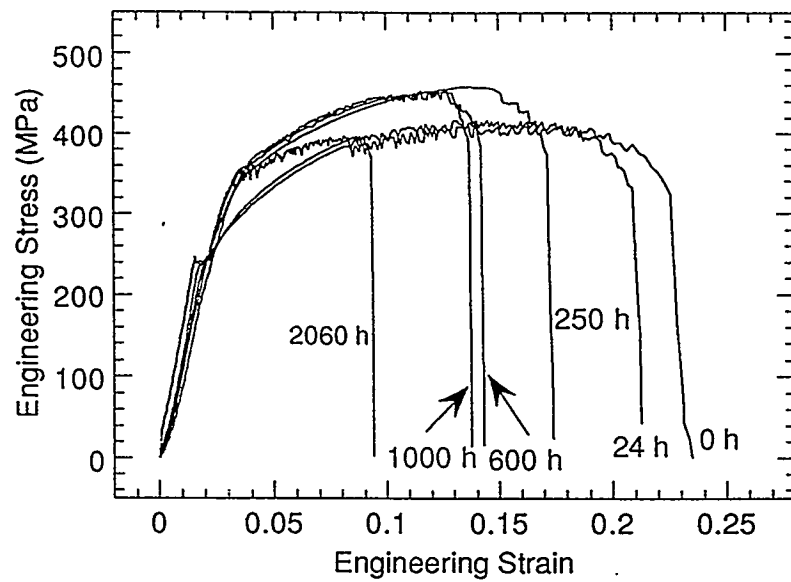
Figure 5. Effect of preoxidation at 500°C on stress-strain behavior of V-5Cr-5Ti alloy tested at 500°C in air at a strain rate of 1.75×10^{-4} s^{-1}.
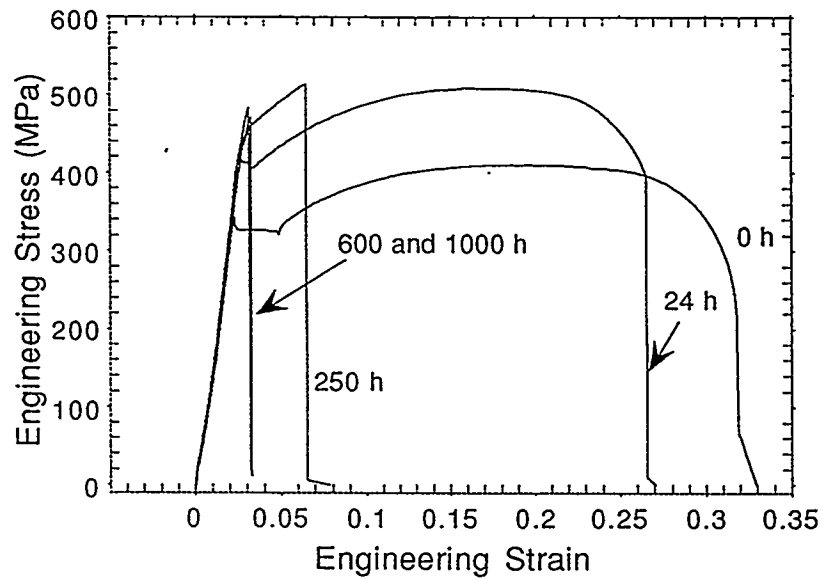

Figure 6. Effect of preoxidation at 500°C on stress-strain behavior of V-5Cr-5Ti alloy tested at room temperature in air at a strain rate of 1.75×10^{-4} s^{-1}.
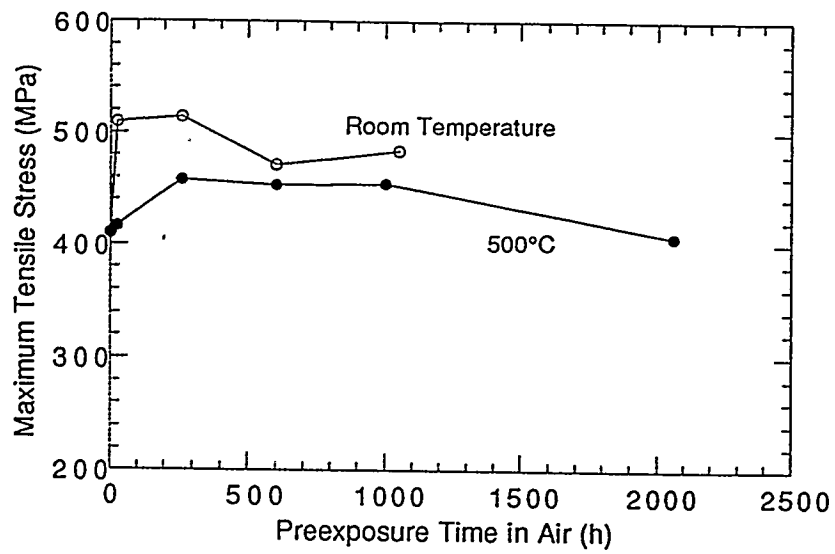
Figure 7. Maximum tensile stress as a function of preexposure time in air for specimens of V-5Cr-5Ti alloy tested in air.
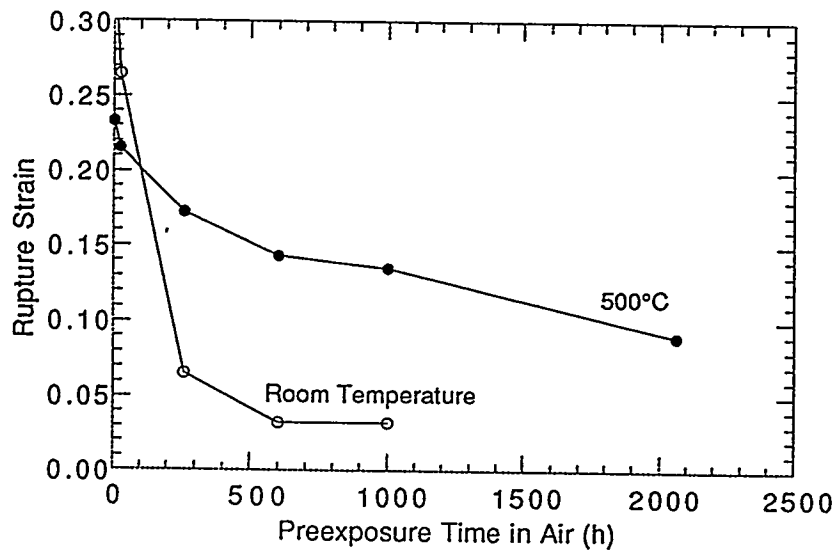
Figure 8. Rupture strain as a function of preexposure time in air for specimens of V-5Cr-5Ti alloy tested in air.

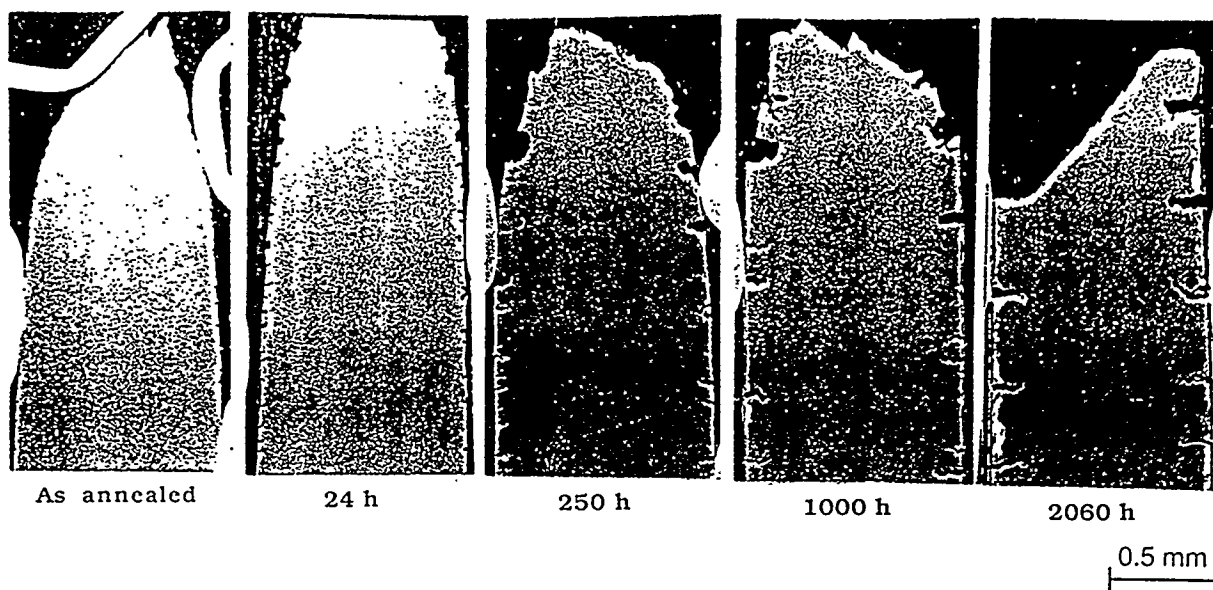As annealed   24 h   250 h   1000 h   2060 h

0.5 mm

Figure 9. Scanning electron photomicrographs of axial sections of V-5Cr-5Ti specimens tensile tested at 500°C in as-annealed condition and after oxidation in air at 500°C for several exposure times

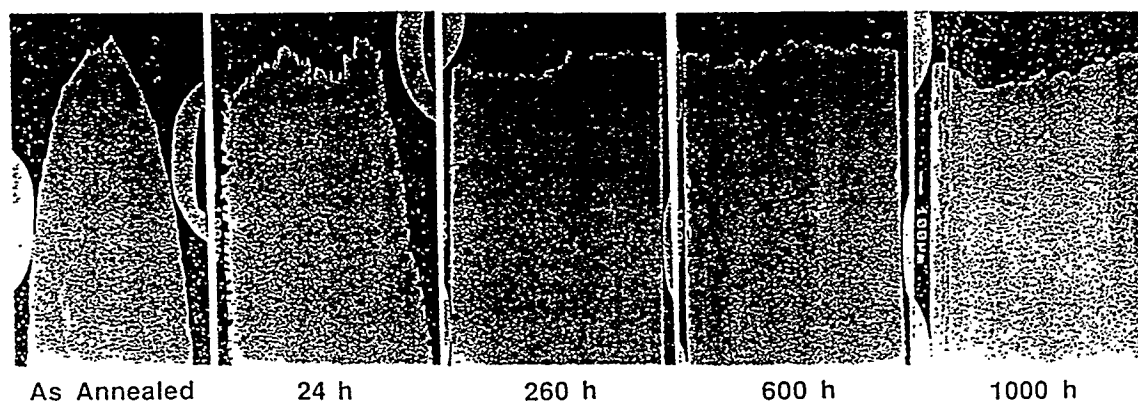As Annealed   24 h   260 h   600 h   1000 h

Figure 10. Scanning electron photomicrographs of axial sections of V-5Cr-5Ti specimens tensile tested at room temperature in as-annealed condition and after oxidation in air at 500°C for several exposure times
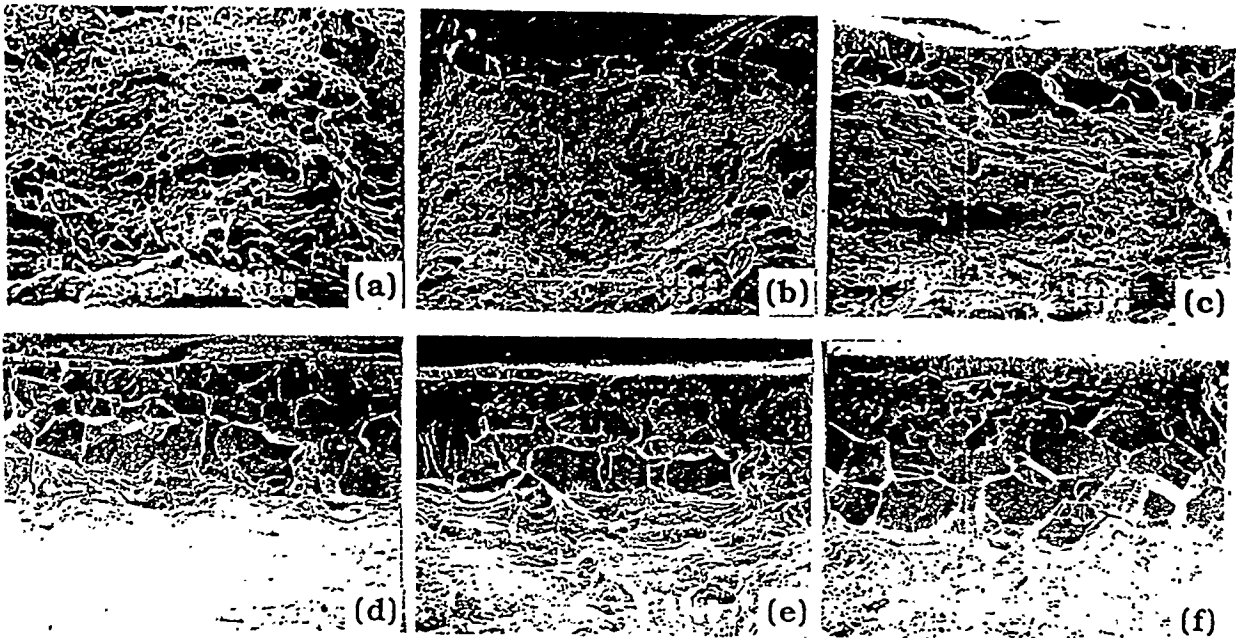
Figure 11. Scanning electron photomicrographs of fracture surfaces of V-5Cr-5Ti specimens tensile tested at 500°C (a) in as-annealed condition and after oxidation in air at 500°C for (b) 24 h, (c) 250 h, (d) 600 h, (e) 1000 h, and (f) 2060 h.
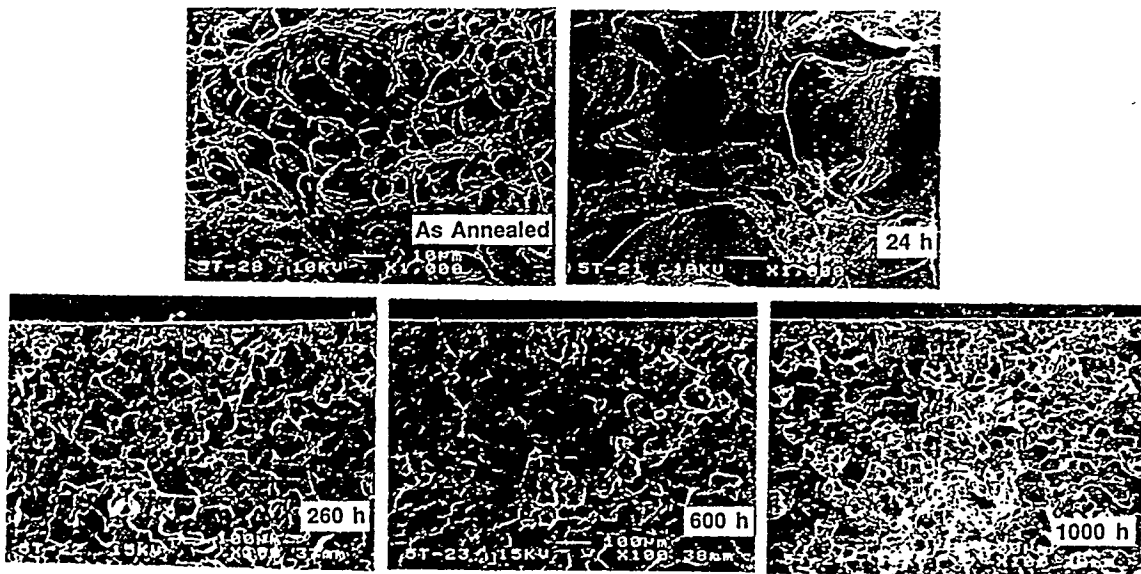

Figure 12. Scanning electron photomicrographs of fracture surfaces of V-5Cr-5Ti specimens tensile tested at room temperature (a) in as-annealed condition and after oxidation in air at 500°C for (b) 24 h, (c) 250 h, (d) 600 h, and (e) 1000 h.
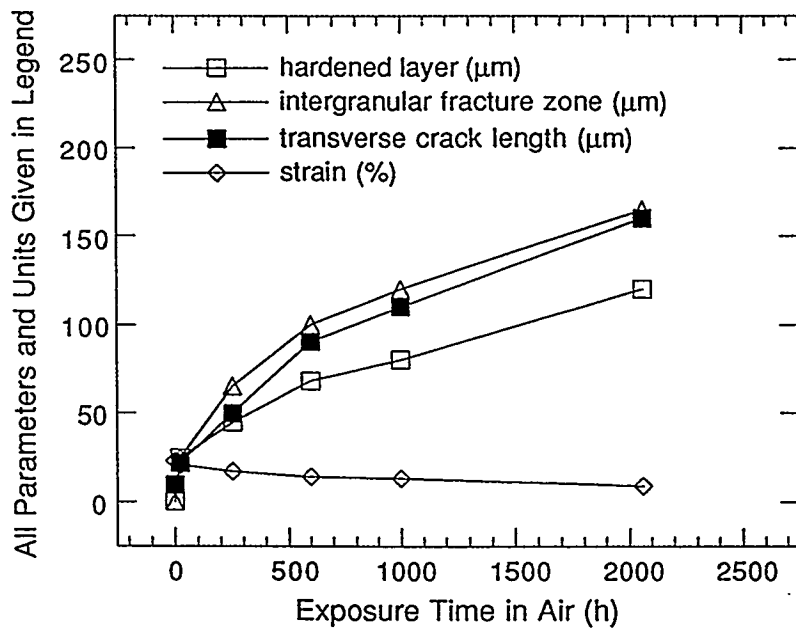
Figure 13. Variation in hardened-layer thickness, intergranular fracture zone depth, transverse crack length, and rupture strain as a function of exposure time at 500°C for V-5Cr-5Ti alloy.

Table 1. Composition of V-5Cr-5Ti alloy[a]

Cr	Ti	Si	Al	B	C	H	N	Nb	O	P	S	V
4.4	5.1	300	200	<5	75	4	25	<50	420	<30	305	Bal[b]

[a] Cr, Ti, and V concentrations are in wt.%; all others are in wppm.
[b] Bal indicates balance.

Table 2. Oxidation, hardness, and fracture data for V-5Cr-5Ti alloy

Exposure time (h)	Calculated oxide thickness[a] (μm)	Measured oxide thickness (μm)	Depth of hardened layer after exposure at 500°C (μm)	Intergranular-fracture zone (μm)		Measured crack length (μm)		Rupture strain	
				RT[b]	500°C	RT[b]	500°C	RT[b]	500°C
0	0	0	0	0	0	0	10	0.322	0.233
24	1.4	1.2	<25	c	25	24	22	0.265	0.215
250[d]	4.6	5.0	45	>500	65	e	50	0.065	0.172
600	7.1	7.1	68	>500	100	e	90	0.032	0.143
1000[d]	9.1	9.0	80	>500	120	e	110	0.032	0.135
2060	13.1	14.0	120	NT[f]	165	NT[f]	160	NT[f]	0.090

[a] Values were calculated using an equation developed from a parabolic fit of all the oxidation data.
[b] RT indicates room temperature.
[c] Fracture is partially ductile and no transition is noted from ductile to brittle fracture.
[d] Exposure times were 260 and 1050 h for the samples tested at room temperature.
[e] Specimen fully embrittled.
[f] NT indicates not tested.